Interaction-Induced Spin Polarization in Quantum Dots

M. C. Rogge,[1,*] E. Räsänen,[2] and R. J. Haug[1]

[1]*Institut für Festkörperphysik, Leibniz Universität Hannover, Appelstr. 2, 30167 Hannover, Germany*
[2]*Nanoscience Center, Department of Physics, University of Jyväskylä, FI-40014 Jyväskylä, Finland*

(Received 29 January 2010; published 20 July 2010)

The electronic states of lateral many-electron quantum dots in high magnetic fields are analyzed in terms of energy and spin. In a regime with two Landau levels in the dot, several Coulomb-blockade peaks are measured. A zigzag pattern is found as it is known from the Fock-Darwin spectrum. However, only data from Landau level 0 show the typical spin-induced bimodality, whereas features from Landau level 1 cannot be explained with the Fock-Darwin picture. Instead, by including the interaction effects within spin-density-functional theory a good agreement between experiment and theory is obtained. The absence of bimodality on Landau level 1 is found to be due to strong spin polarization.

DOI: 10.1103/PhysRevLett.105.046802 PACS numbers: 73.21.La, 72.25.Dc, 73.23.Hk, 73.63.Kv

Spin properties of semiconductor quantum dots (QDs) are of high interest, as the spin of electrons captured in a QD could be used to realize a quantum mechanical bit, the core of future quantum information technologies [1]. In few electron QDs, the electronic spin has been successfully implemented, manipulated, and read (for a review, see [2]). However, in many-electron systems, the dynamics are still not well understood, especially in high magnetic fields.

For QDs with many electrons, the simplest theoretical approximation is done with the so-called constant interaction (CI) model [3,4]. This model uses the single-electron states, most commonly those of a two-dimensional (2D) harmonic potential (Fock-Darwin spectrum [5,6]), and the many-body effects are included just by a constant Coulomb repulsion energy. Despite its simplicity, many features can be qualitatively explained using this model. Among those are the formation of the Landau levels (which allows us to introduce the QD filling factor ν), the crossing of states leading to zigzag patterns, alternating spins, and spin flips. Beyond the CI model, self-consistent calculations successfully described the regularity of zigzag patterns and the electron densities within certain Landau levels [7]. It was found that Landau levels form conductive rings in the dot. Especially for $4 > \nu > 2$, a central region is formed with Landau level 1 ($LL1$) and an outer ring with Landau level 0 ($LL0$), as schematically shown in Fig. 1.

Further investigations on spin blockade and Kondo effect helped to gain knowledge about the spin configuration in the lowest Landau levels (see, e.g., Refs. [8–13]). Calculations by Wensauer *et al.* [14] predicted a spin polarization in $LL0$ at the $\nu = 2$ border as a function of the electron number. This was also found experimentally [11,15]. In addition, collective spin polarization on the highest occupied Landau level has been found in many-electron calculations [13,16,17] indirectly supported by experimental data [10]. However, despite all these results, the level spectrum of many-electron QDs still leaves open questions, and further measurements are required.

Here we concentrate on the spin configuration of both lowest Landau levels in the $4 > \nu > 2$ regime. We present conductance measurements on a lateral QD with approximately 50 electrons in a perpendicular magnetic field. A zigzag pattern of electronic states is found and it is compared with many-body calculations within spin-density-functional theory [18] (SDFT). While the states in $LL0$ show a striking bimodality that can roughly be explained with alternating spin states using the CI model, the states of $LL1$ do not at all follow this model. However, the behavior can be understood with the SDFT calculations showing different spin configurations in the two involved Landau levels as illustrated in Fig. 1. While $LL0$ shows a regular filling of orbitals with alternating spin-up and spin-down electrons as expected, $LL1$ is spin-polarized with spin-up electrons only. Thus, we are able to directly identify interaction-induced spin polarization, which, besides being an interesting many-body phenomenon as such, might be exploited in quantum Hall devices and spintronics.

The sample is made on a GaAs/AlGaAs heterostructure using local anodic oxidation [19–21] and electron beam lithography. To allow electronic transport, the QD is connected to two leads, source and drain, as schematically shown in Fig. 1. A side gate is used to tune the QD

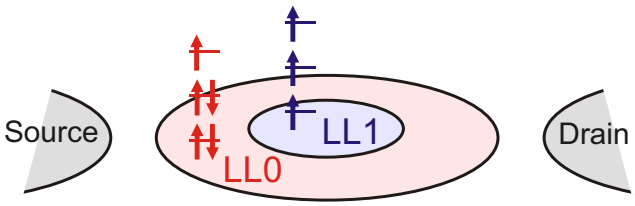

FIG. 1 (color online). Schematic of a single lateral quantum dot connected to two leads (Source and Drain). In a perpendicular magnetic field, Landau levels (LL) appear with a specific spin polarization. Landau level 0 is located at the edge of the dot, Landau level 1 in the center. Arrows show the spin configuration within each Landau level.

potential. Details about the sample preparation and device properties can be found in Ref. [22].

Figure 2(a) shows a measurement of the magnetotransport of the system. The differential conductance G is plotted as a function of the perpendicular magnetic field B and gate voltage V_G. Six Coulomb peaks are visible. The positions of these peaks reflect the chemical potentials of ground-state transitions. These positions can be roughly understood using the CI model. According to this model, the potentials include a fixed Coulomb repulsion energy due to the electrostatic interaction of the electronic charge and a term due to the single-particle excitation spectrum. The single-particle problem is usually calculated describing the confinement of the QD as a 2D harmonic potential, which leads to the Fock-Darwin spectrum [5,6]. In addition, the electronic spin is included via the Zeeman term $g^*\mu_B B s_z$ with the gyromagnetic ratio g^*, the Bohr-magneton μ_B, and the spin quantum number $s_z = \pm 1/2$. According to this model, the pronounced zigzag structures appear as, with increasing magnetic field, different states of the excitation spectrum are energetically favored. The bare excitation spectrum is made visible by removing the constant gaps between Coulomb peaks, as within the CI model these gaps are identical with the Coulomb energy.

We apply this technique in Fig. 2(b). The peak positions of the original Coulomb peaks are transferred to an energy scale. Then a constant energy is removed such that gaps between adjacent Coulomb peaks are eliminated (we did actually remove a gate voltage dependent energy, as the electrostatic electron-electron interaction is reduced with increasing V_G due to changes in the size of the dot. The removed energy is, however, constant as a function of magnetic field, leaving the shapes of Coulomb peaks unaffected). Now states can be followed over several Coulomb peaks (several electron numbers). As a result, a pattern is found with states going up in energy (some marked with $LL1$) and states going down in energy (some marked with $LL0$). These states can be interpreted in terms of Landau levels. States with negative slopes are due to transport via $LL0$, states with positive slopes are due to transport via $LL1$. According to the Fock-Darwin model with spin, for each Landau level there should be a pairing of every two lines. Two adjacent peaks use the same orbital state with opposite spin. Indeed such a pairing is visible for $LL0$ but not for $LL1$.

In order to analyze this behavior in detail, for each Landau level the energy distances between adjacent peaks from Fig. 2(b) are plotted in Fig. 3(a). The distances for $LL0$ (triangles) show the expected bimodal behavior due to the electronic spin. The data can be fitted (dashed lines) using the Fock-Darwin model with confinement strength $\hbar\omega_0 = 1.83$ meV and $g^* = -0.71$. The corresponding Fock-Darwin spectrum using these parameters is shown in Fig. 3(b) around the chemical potential μ_{46} (black trace). Spin-up and spin-down states are shown as solid and dotted lines, respectively. However, the large negative value for the g^* factor (the sign is given by the peak amplitudes due to spin blockade [10]) is a first hint, that the description with the CI model is incomplete. Because of the confinement potential of the dot, the g^* factor should

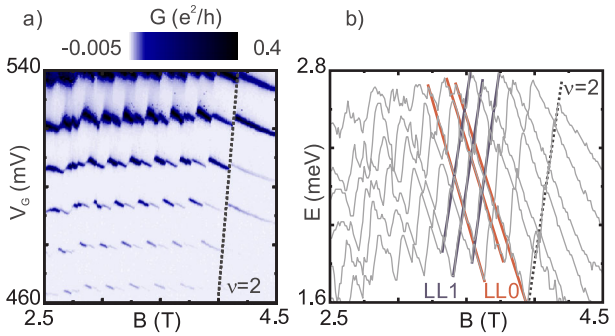

FIG. 2 (color online). (a) Differential conductance G as a function of magnetic field B and gate voltage V_G. Six Coulomb peaks are visible showing a pronounced zigzag pattern. (b) The peak positions are transferred to an energy scale with the Coulomb energy removed. A cross pattern is found with states going down in energy with increasing field ($LL0$) and states going up in energy ($LL1$).

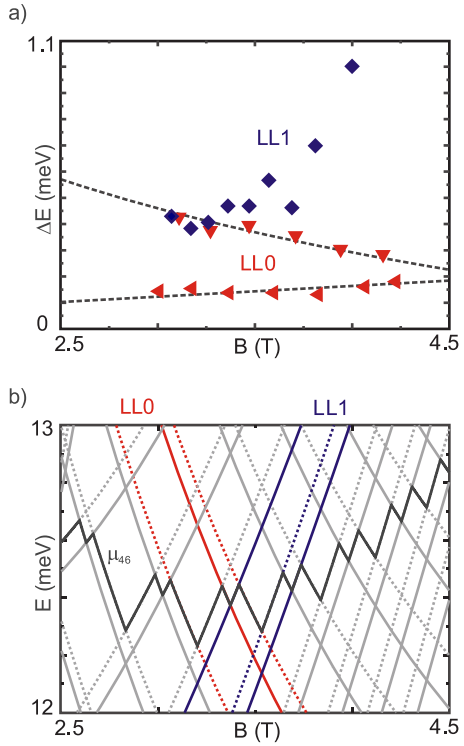

FIG. 3 (color online). (a) Measured energetic peak distances for states in $LL0$ (triangles) and in $LL1$ (diamonds). The distances for $LL0$ show a bimodal behavior due to spin and can be fitted with the Fock-Darwin model (dashed lines, $\hbar\omega_0 = 1.83$ meV, $g^* = -0.71$). The Fock-Darwin spectrum using these parameters is shown in (b). Values for $LL1$ [diamonds in (a)] cannot be explained with the Fock-Darwin spectrum.

be more positive than the one of −0.44 for bulk GaAs. And finally, the description with the CI model is completely insufficient, when data from $LL1$ are included. Within the Fock-Darwin model, the energetic distances do not depend on Landau level, but they should be identical for $LL0$ and $LL1$. This is obviously not the case. In contrast to the Fock-Darwin spectrum [Fig. 3(b)] the measured values for $LL1$ [diamonds in Fig. 3(a)] do not show a bimodal behavior. Moreover, the values are larger as for $LL0$ and increase nonlinearly with magnetic field. Thus a more sophisticated approach is needed including electron-electron interactions that go beyond the CI model.

In the many-body approach we consider the 2D N-electron Hamiltonian

$$H = \frac{1}{2m^*}\sum_{i=1}^{N}[\mathbf{p}_i + e\mathbf{A}(\mathbf{r}_i)]^2 + \sum_{i<j}^{N}\frac{e^2}{4\pi\epsilon_0\epsilon|\mathbf{r}_i - \mathbf{r}_j|} + \sum_{i=1}^{N}[V_{\text{ext}}(\mathbf{r}_i) + E_{z,i}], \quad (1)$$

where $\mathbf{A}$ is the external vector potential (in symmetric gauge) of the homogeneous, perpendicular magnetic field $\mathbf{B} = B\hat{z}$, and the last two terms correspond to the external potential in the harmonic approximation $V_{\text{ext}}(r) = m^*\omega_0^2 r^2/2$ with $\hbar\omega_0 = 4$ meV, and the Zeeman energy $E_z = g^*\mu_B B s_z$, respectively. We note that the 2D modeling of quasi-2D QDs has been well established (for discussion on this topic see, e.g., Ref. [23]). We apply here the conventional effective-mass approximation with the GaAs material parameters: $m^* = 0.067$ and $\epsilon^* = 12.4$. For the gyromagnetic ratio we have chosen $g^* = -0.30$. The scalar approximation for g^* is valid in our system exposed to a perpendicular, static, and uniform magnetic field. The situation is different in epitaxial QDs where effects of anisotropy might be significant [24].

We solve the ground-state energies associated with the 2D N-electron Hamiltonian (1) by applying SDFT [18] in the collinear-spin representation. We note that the external vector potential is retained in the corresponding Kohn-Sham Hamiltonian. To approximate the exchange-correlation energy E_{xc} we use the 2D local spin-density approximation with a parametrization of the correlation energy in the homogeneous 2D electron gas by Attaccalite *et al.* [25]. For total-energy calculations on quasi-2D QDs, SDFT with the 2D local spin-density approximation has been shown to be a reliable scheme in comparison with quantum Monte Carlo calculations, even in relatively high magnetic fields [13,17,26]. Furthermore, it has been found that the current-SDFT [27] (with the local-vorticity approximation) does not lead to a considerable improvement over the SDFT results [26]. In the numerical calculations we apply the OCTOPUS code package [28] which allows using arbitrary external potentials in arbitrary dimensions (1D, 2D, and 3D).

Figure 4(a) shows the chemical potentials $\mu_N = E_N - E_{N-1}$ of the SDFT calculations for $N = 46\ldots48$. The gaps between adjacent Coulomb peaks are removed the same way as in Fig. 2(b). The resulting energy-level distances extracted from the chemical potentials are shown in Fig. 4(b). For $LL1$ we find a clear single mode, whereas $LL0$ has a bimodal behavior as a function of B. This is in a good qualitative agreement with the experimental result in Fig. 3(a).

To analyze the physics behind the energy-level spacings, we focus in the following on the spin configurations given by the SDFT calculations. Their connection to the chemical potentials is shown in Fig. 5. A typical portion of a Coulomb peak in the zig-zag regime is shown together with the spin configurations for both Landau levels for the adjacent regions of constant electron number. $LL0$ shows alternating spin filling resulting in the bimodality of peak sections with negative slopes. The bimodality is due to the energy difference in adding an electron with spin up to a new orbital compared with adding an electron with spin down to a half-filled orbital. We note that the energy difference decreases as a function of B. This is due to both the Zeeman effect and the fact that the increasing

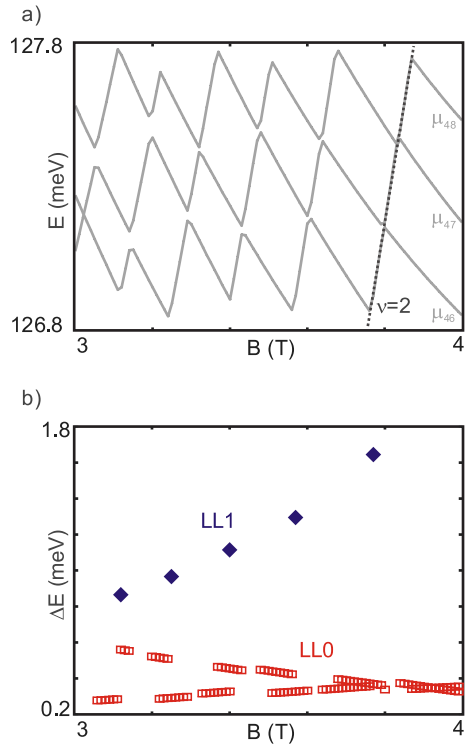

FIG. 4 (color online). Results of the SDFT calculations: (a) chemical potentials μ_{46}, μ_{47}, and μ_{48} without Coulomb energy. As in the experiment, a cross pattern is found. (b) Energetic distances for the two Landau levels. The data qualitatively fit to the measurements. For $LL0$ a bimodal behavior is found (squares). The values for $LL1$ (diamonds) increase with increasing field and do not show a bimodality.

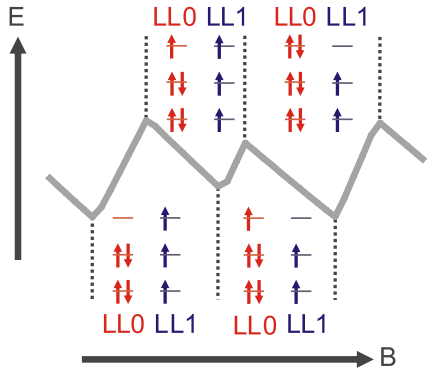

FIG. 5 (color online). Spin configuration resulting from the SDFT calculations for a typical section of the zigzag pattern. While electrons in $LL0$ are filled in regularly with alternating spin, $LL1$ is spin polarized with electrons having spin up only.

magnetic confinement brings the energy states in $LL0$ closer to each other, so that the energy in occupying a new orbital decreases with respect to the filling of a half-filled orbital (costing Coulomb energy).

In contrast with the situation for $LL0$, the higher Landau level ($LL1$), corresponding to peak sections with positive slopes in Figs. 4 and 5, is completely spin-polarized with spin up. Thus, the filling mechanism is always the same and no bimodality is found. The single mode goes up in energy due to the effective increase in the level spacings as a function of B, i.e., $LL1$ becomes more compact, so that the filling of the spin-up orbitals becomes energetically more costly.

We point out that the qualitative features in Figs. 4 and 5 are stable with respect to the values chosen for the gyromagnetic ratio. The reason behind the strong spin polarization of $LL1$ is the high density of states close to the Fermi energy leading to collective, local ferromagnetism familiar from the Stoner effect [29] and Hund's rule. Energetically, this many-body transition corresponds to gaining electronic exchange at the expense of kinetic energy in occupying higher levels. Similar behavior corresponding to the formation of ''spin droplets'' has been predicted by quantum Monte Carlo and SDFT calculations on QDs, indirectly supported by the experimental data of Coulomb-blockade peak positions [13]. It was concluded that the spin-droplet formation requires a relatively large number of electrons ($N \gtrsim 30$) and considerable strength of electron-electron interactions. These conditions are fulfilled by our device, and hence the Landau-level distances visible in our excitation spectra can be considered as a direct and distinct evidence of the spin polarization on the highest occupied Landau level.

To conclude, we analyzed the spin configuration of a single quantum dot containing approximately 50 electrons. In high magnetic fields electronic states were investigated for the two lowest Landau levels. For $LL0$ distances in the excitation spectra show a bimodal behavior, while for $LL1$ only one mode appears. This is explained with two different spin configurations in the two Landau levels. While there is no spin polarization in $LL0$, $LL1$ is completely spin polarized. This is a direct confirmation of the interaction-induced collective spin polarization in quantum dots. The observed and quantified phenomenon provides possibilities for spin manipulation in, e.g., quantum Hall devices such as point contacts, as well as direct applications in spintronics.

This work has been supported by BMBF via nanoQUIT, QUEST, and the Academy of Finland.

*rogge@nano.uni-hannover.de

[1] D. Loss and D. P. DiVincenzo, Phys. Rev. A **57**, 120 (1998).
[2] R. Hanson *et al.*, Rev. Mod. Phys. **79**, 1217 (2007).
[3] C. W. J. Beenakker, Phys. Rev. B **44**, 1646 (1991).
[4] U. Meirav and E. B. Foxman, Semicond. Sci. Technol. **11**, 255 (1996).
[5] V. Fock, Z. Phys. **47**, 446 (1928).
[6] C. G. Darwin, Math. Proc. Cambridge Philos. Soc. **27**, 86 (1931).
[7] P. L. McEuen *et al.*, Phys. Rev. B **45**, 11419 (1992).
[8] M. Stopa *et al.*, Phys. Rev. Lett. **91**, 046601 (2003).
[9] M. Keller *et al.*, Phys. Rev. B **64**, 033302 (2001).
[10] M. Ciorga *et al.*, Phys. Rev. B **61**, R16315 (2000).
[11] M. C. Rogge, C. Fühner, and R. J. Haug, Phys. Rev. Lett. **97**, 176801 (2006).
[12] M. C. Rogge *et al.*, New J. Phys. **8**, 298 (2006).
[13] E. Räsänen *et al.*, Phys. Rev. B **77**, 041302 (2008).
[14] A. Wensauer, M. Korkusinski, and P. Hawrylak, Phys. Rev. B **67**, 035325 (2003).
[15] M. Ciorga *et al.*, Phys. Rev. Lett. **88**, 256804 (2002).
[16] A. Harju, H. Saarikoski, and E. Räsänen, Phys. Rev. Lett. **96**, 126805 (2006).
[17] H. Saarikoski *et al.*, Phys. Rev. B **78**, 195321 (2008).
[18] For a review on density-functional theory, see, e.g., R. M. Dreizler and E. K. U. Gross, *Density Functional Theory* (Springer-Verlag, Berlin, 1990).
[19] M. Ishii and K. Matsumoto, Jpn. J. Appl. Phys. **34**, 1329 (1995).
[20] R. Held *et al.*, Appl. Phys. Lett. **73**, 262 (1998).
[21] U. F. Keyser *et al.*, Appl. Phys. Lett. **76**, 457 (2000).
[22] M. C. Rogge *et al.*, Appl. Phys. Lett. **85**, 606 (2004).
[23] S. Pittalis, E. Räsänen, and C. R. Proetto, Phys. Rev. B **81**, 115108 (2010).
[24] G. Salis *et al.*, Phys. Rev. B **64**, 195304 (2001).
[25] C. Attaccalite *et al.*, Phys. Rev. Lett. **88**, 256601 (2002).
[26] H. Saarikoski *et al.*, Phys. Rev. B **67**, 205327 (2003).
[27] G. Vignale and M. Rasolt, Phys. Rev. Lett. **59**, 2360 (1987).
[28] A. Castro *et al.*, Phys. Status Solidi B **243**, 2465 (2006).
[29] E. C. Stoner, Proc. R. Soc. A **165**, 372 (1938).